Folate-mediated intracellular drug delivery increases the anticancer efficacy of nanoparticulate formulation of arsenic trioxide

Haimei Chen,[1] Richard Ahn,[1] Jeroen Van den Bossche,[2] David H. Thompson,[2] and Thomas V. O'Halloran[1]

[1]Department of Chemistry, Chemistry of Life Processes Institute, Northwestern University, Evanston, Illinois and [2]Department of Chemistry, Purdue University, West Lafayette, Indiana

Abstract

Arsenic trioxide (As_2O_3) is a frontline drug for treatment of acute promyelocytic leukemia and is in clinical trials for treatment of other malignancies, including multiple myeloma; however, efforts to expand clinical utility to solid tumors have been limited by toxicity. Nanoparticulate forms of As_2O_3 encapsulated in 100-nm-scale, folate-targeted liposomes have been developed to lower systematic toxicity and provide a platform for targeting this agent. The resultant arsenic "nanobins" are stable under physiologic conditions but undergo triggered drug release when the pH is lowered to endosomal/lysosomal levels. Cellular uptake and antitumor efficacy of these arsenic liposomes have been evaluated in folate receptor (FR)–positive human nasopharyngeal (KB) and cervix (HeLa) cells, as well as FR-negative human breast (MCF-7) tumor cells through confocal microscopy, inductively coupled plasma mass spectroscopy, and cytotoxicity studies. Uptake of folate-targeted liposomal arsenic by KB cells was three to six times higher than that of free As_2O_3 or nontargeted liposomal arsenic; the enhanced uptake occurs through folate-mediated endocytosis, leading to a 28-fold increase in cytotoxicity. In contrast, tumor cells with lower FR density on the surface (HeLa and MCF-7) showed much less uptake of the folate-targeted drug and lower efficacy. In cocultures of KB and MCF-7 cells, the folate-targeted arsenic liposomes were exclusively internalized by KB cells, showing high targeting specificity. Our studies further indicate that folate-targeted delivery of As_2O_3 with coencapsulated nickel(II) ions (as a nontoxic adjuvant) potentiates the As_2O_3 efficacy in relatively insensitive solid tumor–derived cells and holds the promise of improving drug therapeutic index. [Mol Cancer Ther 2009;8(7):1955–63]

Introduction

Arsenic trioxide (As_2O_3) is a potent clinical agent for the treatment of acute promyelocytic leukemia and is rapidly moving toward designation as a frontline agent (1, 2). It also shows significant activity in relapsed/refractory multiple myeloma (3). The mechanism of action is not fully understood; however, As_2O_3 is involved in induction of differentiation, apoptosis, and angiogenesis (3). Recent studies of As_2O_3 show anticancer activity against a variety of solid tumor models and tumor cell lines, including liver, gastric, ovarian, cervical, breast, prostate, renal, and bladder cancer (4–6). Clinical response of solid tumors to As_2O_3 in many cases, however, has been poor compared with that of hematologic cancers, such as acute promyelocytic leukemia (4, 7), and much higher As_2O_3 dosages are required for solid tumors (8). High doses are accompanied by severe side effects, including peripheral neuropathies, liver failure, and cardiac toxicity, thus limiting their clinical utility (4, 9). Previous pharmacokinetic studies have shown that plasma arsenic is eliminated rapidly with a half-life of ~12 hours after i.v. administration (10, 11), which may partially account for the limited activity of As_2O_3 in solid tumors. To improve the therapeutic index of the drug and expand its clinical utility to solid tumors, an effective delivery system is needed that can increase its accumulation at tumor sites, diminish off-target toxicity, and extend the circulation time of the active agent in blood (12). Encapsulation in liposomes can improve the therapeutic efficacy of numerous agents by reducing their side effects and increasing the drug concentration in tumors through the enhanced permeability and retention effect (13). Liposomal doxorubicin (Doxil), for instance, has an improved therapeutic index and safety profile over its parent drug, doxorubicin, in the clinic (14); however, analogous preparations of liposomal As_2O_3 face a number of challenges.

Instability has been a limiting feature in the few published accounts of liposomal or polymeric carriers for As_2O_3: substantial amounts of the drug are lost within a few hours under physiologic conditions or over a few days under storage conditions (15, 16). In neutral aqueous solutions of As_2O_3, the uncharged $As(OH)_3$ species (which readily diffuses across lipid membranes) is predominant (17, 18). Recently, we have developed a novel process for

Received 1/19/09; revised 4/6/09; accepted 4/14/09; published OnlineFirst 6/30/09.

Grant support: NIH grants GM054111 and GM087016, Center of Cancer Nanotechnology Excellence grant U54CA119341, CDMRP Breast Cancer Research Program grants BC073413 and BC076723, and Robert H. Lurie Comprehensive Cancer Center Core Grant P30CA060553.

The costs of publication of this article were defrayed in part by the payment of page charges. This article must therefore be hereby marked *advertisement* in accordance with 18 U.S.C. Section 1734 solely to indicate this fact.

Requests for reprints: Thomas V. O'Halloran, Department of Chemistry, Chemistry of Life Processes Institute, Northwestern University, Evanston, IL 60208. Phone: 847-491-5060. Fax: 847-491-7713. E-mail: t-ohalloran@northwestern.edu

doi:10.1158/1535-7163.MCT-09-0045

encapsulating nanoparticulate forms of As_2O_3 (18) into 100-nm liposomes with high density (270 mmol/L), excellent retention, and long shelf life (>6 months at 4°C). The method allows As_2O_3 and coencapsulated metal ions to form pH-sensitive nanoparticles within liposomes. Importantly, the pH dependence of the nanoparticle assembly enables these liposomes to unload the drug cargo when the pH is lowered to 6 or 5, as encountered in cellular endosomes and lysosomes (19, 20). Lipid encapsulation further reduces the toxicity of the nanoparticulate As_2O_3 *in vitro* (18). These novel arsenic liposomes present a platform for subsequent conjugation with targeting ligands, such as folic acid and antibodies, which would further enhance tumor uptake. The vitamin folic acid (FA) has a high binding affinity to folate receptors (FR) on the cell surface of many human tumors (21). FR is a tumor marker because it is highly overexpressed in malignant tissues of epithelial origin relative to normal tissues (21). Folic acid has hence emerged as an effective targeting ligand for selective delivery of attached imaging and therapeutic agents to cancer tissues (22).

In this study, we have applied the nanoparticulate formation process (18) to coencapsulate As_2O_3 with transition metal ions (Ni^{2+} and Co^{2+}) into 100-nm folate-targeted liposomes, the bilayer of which contains a small amount (0.3 mol%) of DSPE-PEG_{3350}-folate [i.e., folic acid conjugated with polyethyleneglycol (MW 3350)–derivatized distearoylphosphatidylethanolamine]. This assembly is shown to be robust and to undergo triggered drug release under mildly acidic conditions. Confocal microscopy, quantitative drug analysis, and cytotoxicity studies reveal that these folate liposomal arsenic agents are efficiently taken up by tumor cells in a receptor-mediated process and have significantly enhanced anticancer efficacy relative to the parent drug As_2O_3.

Materials and Methods

Materials

Dipalmitoylphosphatidylcholine (DPPC), 1,2-dipalmitoyl-*sn*-glycero-3-phosphoethanolamine-*N*-(Lissamine rhodamine B sulfonyl; ammonium salt; DPPE-Rh), and 1,2-dipalmitoyl-*sn*-glycero-3-phosphoethanolamine-*N*-[methoxy (polyethylene glycol)-2000] (ammonium salt; DPPE-PEG_{2000}) were purchased from Avanti Polar Lipids. 1,2- Distearoyl-*sn*-glycero-3-phosphoethanolamine-*N*-[folate(polyethylene glycol)-3350] (DSPE-PEG_{3350}-Folate) was synthesized as previously reported (23). Cholesterol (Chol), nickel(II) acetate [$Ni(OAc)_2$], cobalt(II) acetate [$Co(OAc)_2$], sodium chloride, acetic acid, folic acid, paraformaldehyde, HEPES, MES, and Sephadex G-50 were obtained from Sigma. RPMI 1640 was from Invitrogen-Life Technologies. Eagle's MEM and fetal bovine serum (FBS) were from the American Type Culture Collection (ATCC). L-Glutamine, penicillin-streptomycin, and PBS were from MEDIATECH. Folate binding protein antibody (anti-LK26) was from Abcam, Inc., and Alexa Fluor 488 goat anti-mouse IgG was from Invitrogen.

Liposome Preparation and Arsenic Loading

Liposome compositions used in this study were as follows: (*a*) folate-targeted liposomes, DPPC/Chol/DPPE-PEG_{2000}/DSPE-PEG_{3350}-Folate = 53/45/1.7/0.3 mol%; (*b*) nontargeted liposomes, DPPC/Chol/DPPE-PEG_{2000} = 53/45/2 mol%; (*c*) rhodamine (Rh)-labeled folate-targeted liposomes, DPPC/Chol/DPPE-PEG_{2000}/DSPE-PEG_{3350}-Folate/DPPE-Rh = 52.5/45/1.7/0.3/0.5 mol%; (*d*) Rh-labeled nontargeted liposomes, DPPC/Chol/DPPE-PEG_{2000}/DPPE-Rh = 52.5/45/2/0.5 mol%. The lipid mixtures in chloroform were evaporated using a rotary evaporator and then placed under high vacuum overnight to remove any residual solvent. The resulting dried lipid films were hydrated in 300 mmol/L nickel acetate [$Ni(OAc)_2$] or cobalt acetate [$Co(OAc)_2$] aqueous solutions and subsequently subjected to 10 freeze-and-thaw cycles (freezing in ethanol/dry ice bath and thawing in 50°C water bath). The hydrated liposomes were sequentially extruded at 50°C to 60°C with a manual mini-extruder (Avanti Lipids), through a series of polycarbonate filters of pore size ranging from 0.4 to 0.1 μm. Extruded liposomes were fractionated on Sephadex G-50 columns equilibrated with a buffer composed of 150 mmol/L NaCl and 20 mmol/L HEPES (pH 6.8). The Ni$(OAc)_2$ or $Co(OAc)_2$ encapsulated liposomes with or without folate conjugation, f-Lip(Ni), Lip(Ni), f-Lip(Co), or Lip(Co), were then incubated with a As_2O_3 solution at 50°C for 2.5 h. After cooling to room temperature and removal of extraliposomal As_2O_3 with Sephadex G-50 columns, the concentrations of lipids (P), encapsulated As, and M (Ni or Co) in the excluded fractions were determined with an inductively coupled plasma optical emission spectrometer (ICP-OES; Vista MPX). The molar ratios of As/lipid, M/lipid, and As/M were calculated and used to assess loading efficiency. The As and Ni- or Co-coloaded liposomes with or without folate targeting, f-Lip(Ni, As), Lip(Ni, As), f-Lip(Co, As), or Lip(Co, As), had the molar ratios of 0.45 ± 0.08 As/lipid, 0.60 ± 0.1 M/lipid, and 0.75 ± 0.03 As/M (M = Ni, Co). Because the As and M (Ni or Co) species formed solid $M(HAsO_3)$ nanoparticulates within liposomes (18), we can also express the loading as a total number of moles of As per liter of intraliposomal volume. For 100- to 200-nm-scale liposomes, the encapsulated volume is ~1.5 L/mol phospholipid (24). The 0.45 As/lipid molar ratio of arsenic liposomes corresponds to ~300 mmol/L arsenic within one liposome. Rhodamine (Rh)-labeled liposomes with or without folate targeting had similar loading efficiencies. The mean liposome sizes (115 ± 20 nm) were determined by dynamic light scattering on a Zetasizer-Nano ZS (Malvern Instruments). Visualization of folate-targeted liposomes f-Lip(Ni, As) by transmission electron microscopy is shown in Fig. 1A. Transmission electron microscopy samples were stained with 4% uranyl acetate and air-dried before imaging at 200 kV, magnification ×40,000 (Hitachi HF2000, Hitachi High-Technologies Corporation).

Drug Release Assay

Samples of f-Lip(Ni, As) and f-Lip(Co, As) were kept at 4°C or 37°C at different pH values with lipid concentrations of 1.0 mmol/L. An extraliposomal buffer of 150 mmol/L

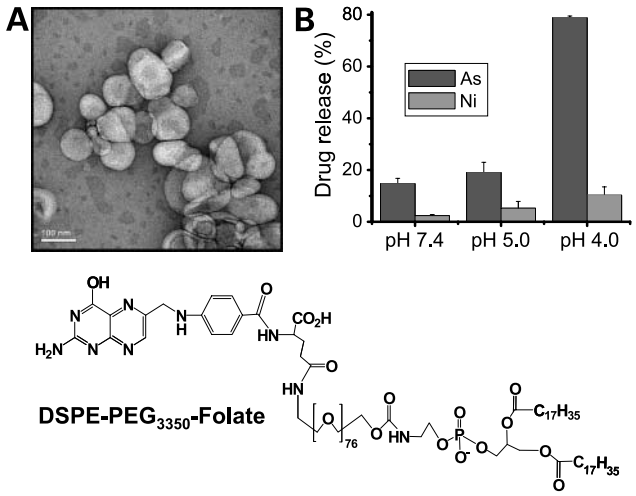

Figure 1. Transmission electron micrograph (**A**) of f-Lip(Ni, As) and its drug release (**B**) at various pH values after 24 h at 37°C. Lipid composition: DPPC/Chol/DPPE-PEG_{2000}/DSPE-PEG_{3350}-Folate = 53/45/1.7/0.3 mol%.

NaCl and 20 mmol/L HEPES was used for maintaining the pH at 7.4; for pH 5.0 or pH 4.0, additional 20 mmol/L MES or acetic acid was added, respectively. For serum samples, liposomes were mixed with FBS in a volume/volume ratio of 2:8 (80% serum) at pH 7.4, 37°C. At various time points, aliquots were applied to a Sephadex G-50 column to remove the arsenic and metal species that had leaked from liposomes. The drug-to-lipid molar ratios in the excluded liposome fractions were determined as described above. The drug release percentage (%) was calculated as $[(r_o - r_i)/r_o] \times 100\%$, where r_o is the initial As(M)-to-lipid molar ratio and r_i the As(M)-to-lipid molar ratio at a specific time point (M = Ni, Co). The results are compared in Fig. 1B and Supplementary Fig. S1.[3] The mean values and SDs (error bars) are based on two independent experiments.

Cell Culture

KB (human nasopharyngeal epidermal carcinoma cells, FR^+), HeLa (human cervical carcinoma cells, FR^+), and MCF-7 (human breast carcinoma cells, FR^-) cells were purchased from ATCC and maintained in a humidified atmosphere containing 5% CO_2 at 37°C following the protocols provided by ATCC. Cells were then cultured in folate-deficient RPMI 1640 with 10% FBS and 1% penicillin-streptomycin for a period (KB, 2 wk; HeLa, 2 mo; MCF-7, 24 h) before each experiment.

Flow Cytometry Analysis of FR Expression

Cells were stained with folate binding antibody (anti-LK26; refs. 25, 26) for 30 min at 4°C. Control cells were incubated in medium only. After removal of excess antibody by PBS washing, cells were treated with the secondary antibody, Alexa Fluor 488 goat anti-mouse IgG, incubated for 30 min at 4°C, and washed with PBS. Cells were then suspended in PBS-buffered 0.5% paraformaldehyde for flow cytometry analysis using a Beckman Coulter Epics XL-MCL instrument (Beckman Coulter, Inc.). The fluorescence intensity observed by flow cytometry is correlated to the amount of FR antigen on the cell surface. A histogram of the fluorescence intensity was plotted and the median fluorescence intensity per cell for each cell type, KB, HeLa, and MCF-7, are compared in Supplementary Fig. S2.[3]

Confocal Microscopy for Visualization of Cellular Uptake of Liposomal Arsenic

Cells were plated, 24 to 48 h before each experiment, on 22-mm coverslips inside six-well plates. Cells were exposed to the Rh-labeled liposomes at 37°C for various times at a lipid concentration of 40 μmol/L and an arsenic concentration of 18 μmol/L. After drug medium removal, cells were washed with PBS × 4 and fixed with PBS-buffered 4% paraformaldehyde at 20°C for 7 min, then washed with PBS × 1. Next, the coverslips were mounted on slides coated with PBS. Microscopic visualization of cells was done using a Zeiss confocal laser scanning microscope (Carl Zeiss LSM 510). For rhodamine (Rh), maximum excitation was obtained from the 543-nm line of a He-Ne laser, and fluorescence emission intensities >570 nm were observed using a long-pass barrier filter LP-570. A water immersion objective, C-Apochromat 63 × 1.2 W corr. (Zeiss), was used. Cells were also imaged by light microscopy using differential interference contrast.

Quantitative Analysis of Drug Uptake

Cells were plated, 24 h before each experiment, in six-well plates at 500,000 cells per well. Cells were exposed to 10 μmol/L arsenic as free drug or within liposomes for various times at 37°C. The same Ni and Co concentrations (13 μmol/L) of f-Lip(Ni) and f-Lip(Co) were used as in f-Lip (Ni, As) and f-Lip(Co, As). After washing with PBS to remove nonassociated drugs, cells were released from tissue culture plates with 0.05% trypsin/0.02% EDTA (Invitrogen), followed by 3 × PBS washing (centrifugation, 500 × *g*, 5 min). A sample was taken for cell number determination through Guave ViaCount Assay (27),[4] using a Guava EasyCyte Mini flow cytometer (Guava Technologies). Cell pellets from each well were digested with 100 μL concentrated nitric acid (trace metal grade, Fisher Scientific) for measurement of arsenic (As), nickel (Ni), and cobalt (Co) concentrations, through inductively coupled plasma mass spectroscopy (ICP-MS, X Series II, Thermo Electron). Cell-associated drug was expressed as As (or Ni, Co) atoms per cell. The mean values and SDs are based on three independent experiments.

Cytotoxicity

Cells were plated, 24 h before each experiment, in 48-well plates at a density of 30,000 to 60,000 cells/mL, 0.2 mL per well. Cells were incubated with drugs continuously for 96 h, or exposed to drugs for 3, 12, and 24 h at 37°C, then washed with PBS × 2 and further incubated up to 96 h in drug-free

[3] Supplementary material for this article is available at Molecular Cancer Therapeutics Online (http://mct.aacrjournals.org/).

[4] http://www.guavatechnologies.com/cm/Home.html

medium. The same Ni and Co concentrations of $Ni(OAc)_2$, Lip(Ni), $Co(OAc)_2$, and Lip(Co) were used as in f-Lip(Ni, As) and f-Lip(Co, As). Cell viability was determined by Guave ViaCount (27),[4] using a Guava EasyCyte Mini flow cytometer (Guava Technologies). Cell growth rates were expressed as a function of drug concentration on a logarithmic scale. The IC_{50} values (the drug concentration required for 50% inhibition of cell growth) were determined by fitting to a sigmoidal dose-response curve using Origin 6.0 (Microcal Software, Inc.). The mean values and SDs are based on two to four independent experiments.

Selective Uptake of Folate-Targeted Liposomal Arsenic in KB/MCF-7 Cocultures

KB/MCF-7 cocultures were prepared by plating a mixture of HeLa and MCF-7 cells in folate-deficient medium on 22-mm coverslips inside six-well plates. After 24 h, KB/MCF-7 cocultured cells were exposed to Rh-labeled folate liposomal arsenic [f-Lip(Ni, As)-Rh] at a lipid concentration of 40 μmol/L for 3 h at 37°C, washed, and visualized by light and confocal microscopy (Fig. 2J). The micrographs were compared with those of KB (Fig. 2E) and MCF-7 (Fig. 2I) alone.

Results

Release of Folate-Targeted Liposomal Arsenic

Folate-targeted liposomal arsenic agents were efficiently loaded with a high density of drug, corresponding to an As/lipid = 0.45 molar ratio. The obtained agents were stable under 4°C storage conditions with <2% drug release within 1 week and <20% within 6 months at pH 7.4 (Supplementary Fig. S1A).[3] When f-Lip(Ni, As) was kept at 37°C with

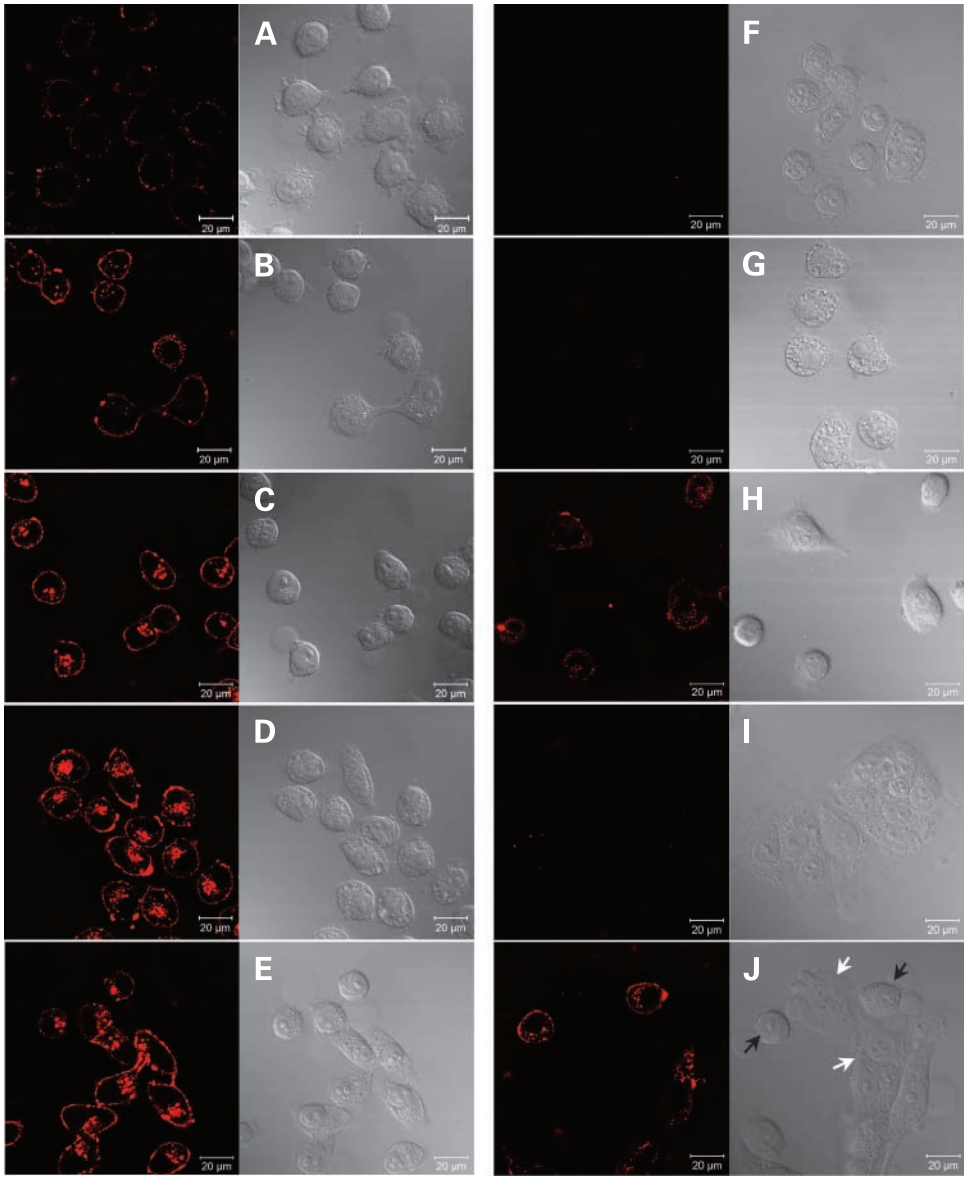

Figure 2. Micrographs showing cellular uptake of f-Lip(Ni, As)-Rh (**A**, 10 min; **B**, 30 min; **C**, 1 h; **D**, 2 h; **E**, 4 h; **F**, 4 h + 2 mmol/L FA) and Lip(Ni, As)-Rh (**G**, 4 h) by KB cells, and of f-Lip(Ni, As)-Rh by HeLa (**H**, 4 h), MCF-7 (**I**, 4 h), and KB/MCF-7 coculture (**J**, 3 h) at 37°C (*black arrow,* KB; *white arrow,* MCF-7). *Left panels,* confocal micrographs; *right panels,* differential interference contrast micrographs.

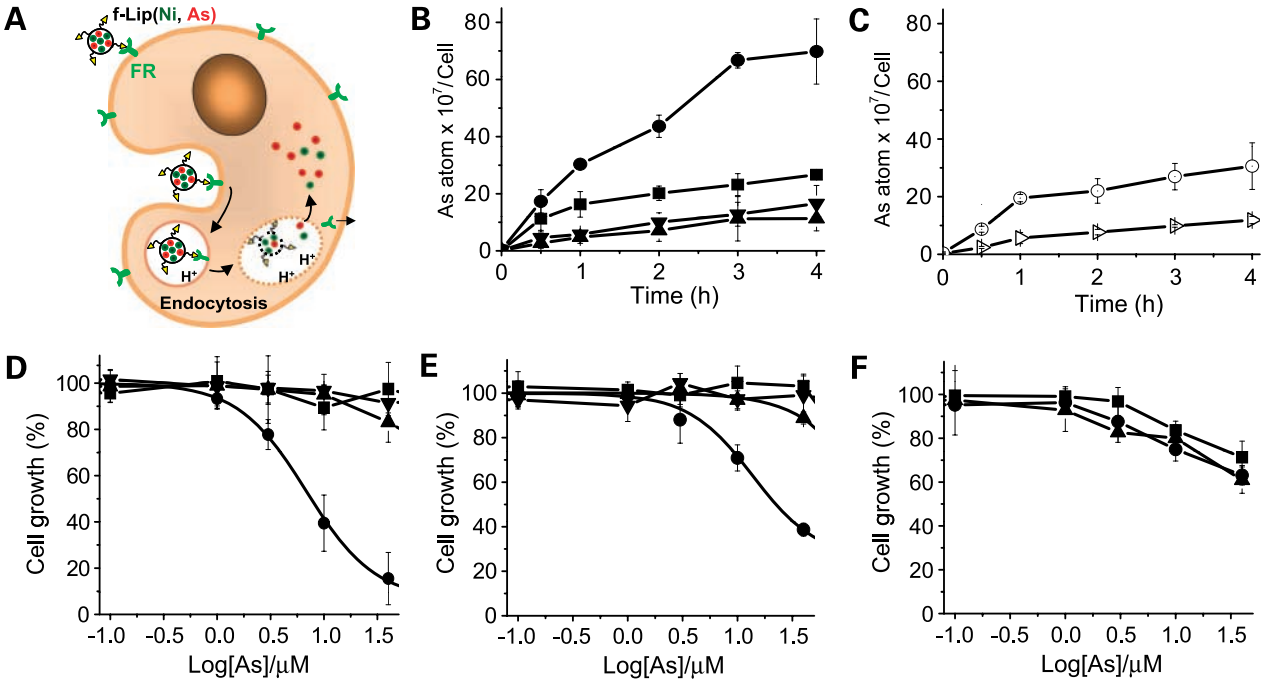

Figure 3. Comparison of cellular arsenic uptake and cytotoxicity of various arsenic formulations. **A,** schematic representation of intracellular uptake of f-Lip(Ni, As) into FR-positive tumor cells. Time dependence of (**B**) KB cellular arsenic uptake of f-Lip(Ni, As) (●), f-Lip(Ni, As) + 2 mmol/L FA (▼), Lip(Ni, As) (▲), and As_2O_3 (■), and of (**C**) cellular arsenic uptake of f-Lip(Ni, As) by HeLa (⊙) and MCF-7 (▷) under the same conditions at 37°C. Cytotoxic effects of f-Lip(Ni, As)(●), f-Lip(Ni, As) + 2 mmol/L FA (▼), Lip(Ni, As) (▲), and As_2O_3 (■) toward KB (**D**), HeLa (**E**), and MCF-7 (**F**), with cells exposed to drugs at 37°C for 3 h, washed by PBS, and further incubated for 93 h in drug-free medium.

80% FBS, 20% arsenic was released after 24 hours (Supplementary Fig. S1C). Drug release is stimulated by lowering the solution pH (Fig. 1B; Supplementary Fig. S1D).[3] After 24 hours at 37°C, 80% arsenic was released from f-Lip(Ni, As) and 95% from f-Lip(Co, As) at pH 4.0, compared with 15% and 13% release at pH 7.4, respectively. For both f-Lip (Ni, As) and f-Lip(Co, As), 20% to 30% of the arsenic was released after 24 hours at pH 5.0.

Cellular Uptake of Folate-Targeted Liposomal Arsenic

Two FR-positive (FR^+) tumor cell lines, KB and HeLa, as well as the FR-negative (FR^-) cell line, MCF-7, were studied for binding of folate liposomal arsenic. FR expression on the cell surface was analyzed by flow cytometry using a folate binding antibody (anti-LK26; refs. 25, 26). Significant FR expression was found for both KB and HeLa cells, but not for MCF-7, with the order of KB > HeLa >> MCF-7 (Supplementary Fig. S2).[3] This result is consistent with the previous FR analysis using [^{3}H]folic acid (28). Cellular association of folate liposomal arsenic was examined by confocal microscopy using rhodamine (Rh)–labeled liposomes. As shown in Fig. 2, binding of f-Lip(Ni, As)-Rh to KB cells in folate-free medium was obvious within a 30-minute exposure (Fig. 2A and B), mainly through surface binding, as indicated by the red fluorescence of Rh on the cell surface. Subsequent liposome internalization and accumulation in the cytosol was observed at 1 hour (Fig. 2C) and became more obvious after 2 hours (Fig. 2D and E), with more red punctuate fluorescence around the nuclei. In contrast, nontargeted Lip(Ni, As)-Rh showed little fluorescence above background, indicating little cellular association at 4 hours (Fig. 2G). For free ligand competition studies, 2 mmol/L folic acid was added, resulting in a dramatic decrease of cellular association (both surface binding and internalization) for f-Lip(Ni, As) (Fig. 2F), indicating folate-mediated endocytosis of the nanoparticulate arsenic agents (Fig. 3A). For HeLa cells, a similar endocytosis process of f-Lip(Ni, As) was observed, but at a lower extent (Fig. 2H), probably due to their lower FR level relative to that of KB cells (Supplementary Fig. S2;[3] ref. 28). FR-negative MCF-7 cells showed no significant association with f-Lip(Ni, As) at 4 hours (Fig. 2I).

In coculture studies, KB cells were mixed with MCF-7 and maintained in folate-free medium. KB cells exhibit a morphology (round and isolated; Fig. 2E) that is easily distinguishable from that of MCF-7 cells (flat and aggregated; Fig. 2I) by light microscopy. These cocultures were exposed to f-Lip(Ni, As)-Rh for 3 hours at 37°C before confocal microscopy studies. We find that a significant amount of folate-liposomal arsenic is taken up by the KB cells but not by MCF-7 cells (Fig. 2J), indicating that the folate ligand mediates selective targeting of liposomal arsenic.

ICP-MS analysis of cellular arsenic levels revealed that f-Lip(Ni, As) uptake by KB cells was rapid over the first 3-hour incubation at 37°C (Fig. 3B). At 3 hours, f-Lip(Ni, As) uptake by KB cells was about six times higher than those of Lip(Ni, As) and f-Lip(Ni, As) + 2 mmol/L FA and three times higher than that of free As_2O_3. For HeLa

Table 1. Cytotoxicity of various arsenic formulations to tumor cells

Cell lines	IC_{50} (As/μmol/L)			
	As_2O_3	Lip(Ni, As)	f-Lip(Ni, As)	f-Lip(Ni, As) + 2 mmol/L FA
KB (FR^+)				
3 h	>200	>200	7.1 ± 3.8	>200
12 h	24.3 ± 7.4	32.4 ± 9.9	3.5 ± 0.2	50.4 ± 26.6
24 h	6.0 ± 0.8	12.1 ± 0.6	2.1 ± 0.1	13.5 ± 1.1
96 h	3.4 ± 0.6	4.4 ± 0.6	1.2 ± 0.4	5.6 ± 0.5
HeLa (FR^+)				
3 h	>200	>200	23.4 ± 2.4	>200
12 h	18.3 ± 5.0	43.2 ± 14.0	9.3 ± 5.7	52.0 ± 5.9
24 h	6.0 ± 0.5	16.6 ± 9.1	5.5 ± 2.2	12.3 ± 0.5
96 h	4.3 ± 0.3	5.7 ± 0.4	1.8 ± 0.6	3.5 ± 0.8
MCF-7 (FR^-)*				
3 h	>100	>100	>100	—
12 h	5.8 ± 0.4	20.9 ± 1.4	15.5 ± 7.7	—
24 h	3.2 ± 0.4	5.9 ± 0.5	5.4 ± 0.3	—

NOTE: Cells were incubated with drugs for a continuous 96 hours or exposed to drugs for 3, 12, and 24 hours at 37°C, then washed and further incubated up to 96 h in a drug-free medium followed by Guava ViaCount assay for IC_{50} measurement. IC_{50} values are based on As concentration (μmol/L). The mean values and SDs are based on two to four independent experiments.

*IC_{50} measurement was not done for a continuous 96-h incubation.

cells, uptake of f-Lip(Ni, As) gradually increased within the first 4-hour period, reaching levels significantly higher than those for Lip(Ni, As), f-Lip(Ni, As) + 2 mmol/L FA, and free As_2O_3 (Supplementary Fig. S3B).[3] For comparison, there were 6.7×10^8 arsenic atoms taken up per KB cell at 3 hours when treated with f-Lip(Ni, As), which is 2.5 times higher than that taken up by HeLa cells (2.7×10^8 arsenic atoms per cell) and 6.8 times higher than that taken up by MCF-7 cells (0.98×10^8 arsenic atoms per cell; Fig. 3B and C).

Folate Targeting Significantly Enhances Cytotoxic Effects of As_2O_3 in a Receptor-Dependent Manner

The cytotoxic effects of various arsenic formulations toward KB, HeLa, and MCF-7 cells in folate-free medium are compared in Table 1 and Fig. 3D to F. At 3 hours, f-Lip(Ni, As) was approximately 28 (for KB cells) and 9 (for HeLa cells) times more cytotoxic than Lip(Ni, As), f-Lip(Ni, As) + 2 mmol/L FA, and free As_2O_3, and showed significant folate-mediated targeting effect. Notably, liposome encapsulation alone generally reduced the cytotoxicity of free As_2O_3 to both KB and HeLa cells (Table 1). After targeting by folate ligands [f-Lip(Ni, As)], the potency of liposomal arsenic was significantly enhanced, with cytotoxicity increased by 28 times (3 hours), 9 times (12 hours), 6 times (24 hours), and 4 times (96 hours) in KB cell cultures, and by 9 times (3 hours), 5 times (12 hours), 3 times (24 hours), and 3 times (96 hours) in HeLa cultures (Table 1). The degree of potentiation of f-Lip (Ni, As) versus Lip(Ni, As) gradually decreased at longer drug exposure times, probably due to nonspecific cellular association of liposomes and/or passive arsenic release, both of which would contribute to the cytotoxicity of nontargeted Lip(Ni, As). For MCF-7 cells, f-Lip(Ni, As) show similar cytotoxic effects to Lip(Ni, As) at 3, 12, and 24 hours (Table 1), without obvious folate-mediated targeting effect. This is consistent with the lowest FR level in MCF-7 cells (Fig. 2I and Supplementary Fig. S2).[3]

Similar Cellular Uptake Efficiencies for f-Lip(Ni, As) and f-Lip(Co, As)

KB cells were exposed to f-Lip(Ni, As), f-Lip(Ni), f-Lip (Co, As), and f-Lip(Co) at 10 μmol/L As and 13 μmol/L Ni or Co for 3 hours at 37°C. Similar levels of cellular uptake of As, Ni, or Co (atoms per cell) were found among different drug formulations (Table 2), consistent with the

Table 2. Comparison of cellular uptake and cytotoxicity of various drug formulations to KB cells

Formulations	Cellular uptake ($\times 10^8$ atoms/cell)			IC_{50} (μmol/L)		
	As	Ni	Co	As	Ni	Co
f-Lip(Ni, As)	5.7 ± 2	10.0 ± 3		7.1 ± 3.8	9.2 ± 4.9	
f-Lip(Ni)		9.5 ± 2			61.4 ± 24	
f-Lip(Co, As)	5.8 ± 2		9.4 ± 4	> 200		>260
f-Lip(Co)			8.7 ± 4			>300

NOTE: Cellular uptake was measured with the aid of ICP-MS after cells were exposed to drugs for 3 hours at 37°C. IC_{50} values were measured after cells were incubated with drugs for 3 hours at 37°C, then washed and further incubated in a drug-free medium for 93 hours, followed by Guava ViaCount assay. IC_{50} values are based on As, Ni, or Co concentration (μmol/L). The mean values and SDs are based on three independent experiments.

confocal microscopy visualization (Supplementary Fig. S4).[3] This indicates that these four drug formulations have similar efficiency of folate-mediated cellular uptake.

Higher Antitumor Potency of f-Lip(Ni, As) than that of f-Lip(Co, As)

KB cells were exposed to various drug formulations for 3 hours at 37°C, washed, and further incubated for 93 hours. F-Lip(Co, As) gave an IC_{50} >200 μmol/L As or 260 μmol/L Co, which is 28 times higher than that of f-Lip(Ni, As) (IC_{50} of 7.1 μmol/L As or 9.2 μmol/L Ni; Table 2 and Supplementary Fig. S5).[3] Before arsenic loading, f-Lip(Ni) showed a slight cytotoxic effect with IC_{50} of 61.4 μmol/L Ni, whereas f-Lip(Co) had an IC_{50} >300 μmol/L Co (Table 2). A similar result was found for HeLa treatments, with f-Lip(Ni, As) being up to nine times more potent than f-Lip(Co, As) at 3 hours (Supplementary Fig. S8A).[3] These results indicate that the nickel component within the folate-targeted arsenic liposome serves as an adjuvant that stimulates the anticancer activity of the arsenic drug.

Discussion

This study shows that nanoparticulate forms of the anticancer drug As_2O_3 can be specifically targeted to cancer cells in a ligand-targeted manner. The nanoparticulate drug is entrapped in folate-tethered liposomes with the aid of coencapsulated transition metal ions and undergoes a folate-mediated endocytosis, leading to highly selective cell killing. This approach significantly increases both the potency and specificity of As_2O_3 to the relatively insensitive solid tumor–derived cells and holds the promise of improving the therapeutic index of the drug and expanding its utility in treatment of a wide variety of cancers.

Stable nanoparticulate formation of liposomal As_2O_3 are efficiently prepared by preloaded liposomes with high concentrations of transition metal acetate salts and subsequent addition of aqueous solutions of As_2O_3 (18). These arsenic "nanobins" have a long shelf life and exhibit attenuated toxicity relative to free As_2O_3 at neutral pH (18). Under mildly acidic conditions such as those found in endosomal/lysosomal compartments, however, these agents undergo triggered arsenic drug release with $As(OH)_3$ (the active species of As_2O_3; ref. 17) diffusing out of liposomes (18). We show here that this arsenic-loaded system is a robust platform for further optimization by conjugation with specific ligands or antibodies for targeting to specific tumors. Folic acid and its derivatives have been used as effective targeting ligands for treatment of certain tumors (22) because FR is often overexpressed in malignant tissues of epithelial origin, such as ovarian carcinomas (29), but not in normal tissues. Folate targeting in our arsenic liposomal system is achieved with DSPE-PEG_{3350}-Folate (Fig. 1) to present the folate ligand on the liposome surfaces. The presence of a small amount (0.1-0.5 mol%) of DSPE-PEG_{3350}-Folate resulted in the efficient FR-dependent uptake of liposomes (30). Here, we used 0.3 mol% amount of DSPE-PEG_{3350}-Folate, which was added to the original mixture of lipids. After the lipid film was hydrated in a 300 mmol/L $Ni(OAc)_2$ or $Co(OAc)_2$ aqueous solution and then extruded through 100-nm filters, and the extraliposomal metal ion was removed by gel filtration, a solution of As_2O_3 was added and allowed to actively load into these folate-targeted liposomes through diffusion of the neutral $As(OH)_3$ species across the liposomal membrane. We show that the presence of folate ligands did not impair the loading efficiency and stability of liposomal arsenic: high encapsulation efficiency was achieved with As/lipid of 0.45 molar ratio, corresponding to ~300 mmol/L arsenic within one single folate liposome. The resulting folate-modified agents are homogenous and stable under storage conditions (Fig. 1A). Although the folate liposomal arsenic drug was stably retained (Supplementary Fig. S1A)[3] with a long shelf life (<20% release within 6 months at 4°C and pH 7.4), its release was facilitated by lowering the pH to 5 (Fig. 1B and Supplementary Fig. S1D),[3] a pH close to that found in endocytic compartments of the folate-mediated endocytosis pathway (19, 20, 31).

We further found that these folate-targeted arsenic-loaded liposomes have efficient cellular uptake and anticancer activities with high specificity. Confocal microscopy studies indicate rapid binding of f-Lip(Ni, As) through surface receptor association followed by endocytosis for KB (FR^+) and HeLa (FR^+) cells, but not MCF-7 (FR^-) cells (Fig. 2). In addition, f-Lip(Ni, As) seemed to be internalized exclusively by KB cells in KB/MCF-7 cocultures (Fig. 2J), suggesting that folate liposomes can facilitate *in vivo* targeting of As_2O_3 drugs to tumors whose cells overexpress FRs, while preventing the killing of adjacent FR-negative cells in normal tissues. Quantitative analysis further revealed the rapid uptake and substantial accumulation of arsenic within KB and HeLa cells, but not MCF-7 cells when treated with f-Lip(Ni, As) for 3 hours at 37°C (Fig. 3B and C), largely consistent with confocal microscopy findings (Fig. 2). Notably, Lip(Ni, As) had approximately three times lower uptake than free As_2O_3 at 3 hours by KB and HeLa cells (Fig. 3B; Supplementary Fig. S3B).[3] As expected, liposome encapsulation reduced the cellular membrane permeability of As_2O_3; however, when such drug-loaded liposomes are linked with folate ligands [f-Lip(Ni, As)] and delivered into tumor cells through folate-mediated endocytosis (Fig. 2E and H), an efficient intracellular unloading of liposomal contents [$As(OH)_3$ and metal ions] can be achieved (19, 20, 31) and thus accelerate biological actions of drugs (Fig. 3A). This may account for the significantly enhanced cytotoxicity (up to 28-fold for KB and 9-fold for HeLa) of f-Lip(Ni, As) relative to those of free As_2O_3 and Lip(Ni, As) (Table 1).

We also found that the nature of the coencapsulated transition metal ions inside folate liposomes can influence the efficacy of As_2O_3 (Table 2 and Supplementary Fig. S8).[3] After a 3-hour exposure at 37°C, f-Lip(Ni, As) were 28 and 9 times more cytotoxic than f-Lip(Co, As) toward KB and HeLa cells, respectively, although the cellular uptake efficiency of f-Lip (Co, As) was very close to that of f-Lip(Ni, As) (Table 2). Given that both f-Lip(Ni, As) and f-Lip(Co, As) exhibit similar extents of drug release at low pHs (Fig. 1B; Supplementary Fig. S1D),[3] the much higher cytotoxicity of f-Lip(Ni, As)

versus f-Lip(Co, As) indicates that when the agents are simultaneously delivered through folate-mediated endocytosis (Fig. 3A), Ni^{2+} ions enhance the biological activity of As_2O_3 relative to Co^{2+}.

Other agents are known to enhance the antitumor activities of As_2O_3, including ascorbic acid (32), all-*trans*-retinoic acid (33), L-buthionine-sulfoximine (34), and docosahexaenoic acid (35, 36). These agents are thought to act through modulation of the cellular glutathione (GSH) redox system, which is a critical component of the cellular response to oxidative stress and the induction of apoptosis (9, 37). Agents that lower GSH levels are known to potentiate the apoptotic effect of As_2O_3, whereas those preserving or increasing GSH levels can cause a reduction in the apoptotic effect of As_2O_3 (37, 38). Ni^{2+} ions have been reported to lower GSH levels (39–41), whereas Co^{2+} ions are thought to increase it based on a number of *in vitro* and *in vivo* studies (42–44). These findings may be correlated with our observations in this study: Ni^{2+} ions increased the cytotoxic effect of As_2O_3, whereas Co^{2+} ions decreased it (Table 2), after codelivery into tumor cells by folate-targeted liposomes (Fig. 3A). In contrast, such enhancing effects of Ni^{2+} on As_2O_3 cytotoxicity were not found in cells treated with simple aqueous mixtures of As_2O_3 and $Ni(OAc)_2$ (Supplementary Fig. S9)[3] or with nontargeted Lip(Ni, As) (Supplementary Figs. S7 and S8).[3] Furthermore, neither free, nontargeted liposomal $Ni(OAc)_2$ nor empty folate liposomes were toxic within the effective dose range of As_2O_3 (Supplementary Fig. S6),[3] warranting the safety of this approach of codelivering As_2O_3 with the Ni^{2+} adjuvant using folate liposome vesicles to efficiently target specific tumors. These findings emphasize the advantage of targeted liposomes as a system for codelivery of an active agent and a nontoxic adjuvant.

In conclusion, we have shown a promising strategy for targeting As_2O_3 to specific tumor cells using folate-tethered liposomes. As_2O_3 can be stably and efficiently loaded into folate liposomes through transmembrane gradients of transition metal ions (Ni^{2+} and Co^{2+}). The resulting folate liposomal arsenic drugs show higher anticancer efficacy against FR-overexpressing solid tumor cells, which are relatively insensitive to free As_2O_3. The coencapsulated Ni^{2+} ions contribute to retention of the As_2O_3 drug within the liposomal carrier under physiologic situations and modulate pH-triggered drug unloading in endocytic compartments involved in cellular uptake. They also enhance the anticancer activity of As_2O_3. Future preclinical studies will elucidate the role of enhanced permeability and retention and folate-directed targeting *in vivo*. Our results provide a rationale for combined Ni/As therapy in further animal studies through the folate-targeted liposomal codelivery system. This novel targeting system will be extended to treatments of other FR-overexpressing tumors, such as ovarian cancer (29) and lymphoma (45), and to improve the therapeutic profile of the drug.

Disclosure of Potential Conflicts of Interest

No potential conflicts of interest were disclosed.

Acknowledgments

We thank Rebecca Marvin for help with ICP-MS; Dr. R. MacDonald for critical reading of the manuscript; and Sang-Min Lee and Drs. S.T. Nguyen, T.K. Woodruff, and J.E. Burdette for stimulating discussions.

References

1. Zhu J, Chen Z, Lallemand-Breitenbach V, de The H. How acute promyelocytic leukaemia revived arsenic. Nat Rev Cancer 2002;2:705–13.

2. Wang ZY, Chen Z. Acute promyelocytic leukemia: from highly fatal to highly curable. Blood 2008;111:2505–15.

3. Berenson JR, Yeh HS. Arsenic compounds in the treatment of multiple myeloma: a new role for a historical remedy. Clin Lymphoma Myeloma 2006;7:192–8.

4. Dilda PJ, Hogg PJ. Arsenical-based cancer drugs. Cancer Treat Rev 2007;33:542–64.

5. Maeda H, Hori S, Nishitoh H, et al. Tumor growth inhibition by arsenic trioxide (As_2O_3) in the orthotopic metastasis model of androgen-independent prostate cancer. Cancer Res 2001;61:5432–40.

6. Kito M, Matsumoto K, Wada N, et al. Antitumor effect of arsenic trioxide in murine xenograft model. Cancer Sci 2003;94:1010–4.

7. Chen Z, Chen GQ, Shen ZX, et al. Expanding the use of arsenic trioxide: leukemias and beyond. Semin Hematol 2002;39:22–6.

8. Liu B, Pan S, Dong X, et al. Opposing effects of arsenic trioxide on hepatocellular carcinomas in mice. Cancer Sci 2006;97:675–81.

9. Evens AM, Tallman MS, Gartenhaus RB. The potential of arsenic trioxide in the treatment of malignant disease: past, present, and future. Leuk Res 2004;28:891–900.

10. Ni J, Chen G, Shen Z, et al. Pharmacokinetics of intravenous arsenic trioxide in the treatment of acute promyelocytic leukemia. Chin Med J (Engl) 1998;111:1107–10.

11. Wang Z, Zhou J, Lu X, Gong Z, Le XC. Arsenic speciation in urine from acute promyelocytic leukemia patients undergoing arsenic trioxide treatment. Chem Res Toxicol 2004;17:95–103.

12. Allen TM, Cullis PR. Drug delivery systems: entering the mainstream. Science 2004;303:1818–22.

13. Li SD, Huang L. Pharmacokinetics and biodistribution of nanoparticles. Mol Pharm 2008;5:496–504.

14. Gabizon AA. Pegylated liposomal doxorubicin: metamorphosis of an old drug into a new form of chemotherapy. Cancer Invest 2001;19:424–36.

15. Kallinteri P, Fatouros D, Klepetsanis P, Antimisiaris SG. Arsenic trioxide liposomes: encapsulation efficiency and *in vitro* stability. J Liposome Res 2004;14:27–38.

16. Yang Z, Yang M, Peng J. Evaluation of arsenic trioxide-loaded albumin nanoparticles as carriers: preparation and antitumor efficacy. Drug Dev Ind Pharm 2008;34:834–9.

17. Ni Dhubhghaill OM, Sadler PJ. The structure and reactivity of arsenic compounds: biological activity and drug design. Struct Bonding (Berlin) 1991;78:129–90.

18. Chen H, MacDonald RC, Li S, Krett NL, Rosen ST, O'Halloran TV. Lipid encapsulation of arsenic trioxide attenuates cytotoxicity and allows for controlled anticancer drug release. J Am Chem Soc 2006;128:13348–9.

19. Mellman I, Fuchs R, Helenius A. Acidification of the endocytic and exocytic pathways. Annu Rev Biochem 1986;55:663–700.

20. Steinman RM, Mellman IS, Muller WA, Cohn ZA. Endocytosis and the recycling of plasma membrane. J Cell Biol 1983;96:1–27.

21. Sudimack J, Lee RJ. Targeted drug delivery via the folate receptor. Adv Drug Deliv Rev 2000;41:147–62.

22. Low PS, Henne WA, Doorneweerd DD. Discovery and development of folic-acid-based receptor targeting for imaging and therapy of cancer and inflammatory diseases. Acc Chem Res 2008;41:120–9.

23. Gabizon A, Horowitz AT, Goren D, et al. Targeting folate receptor with folate linked to extremities of poly(ethylene glycol)-grafted liposomes: *in vitro* studies. Bioconjug Chem 1999;10:289–98.

24. Haran G, Cohen R, Bar LK, Barenholz Y. Transmembrane ammonium sulfate gradients in liposomes produce efficient and stable entrapment of amphipathic weak bases. Biochim Biophys Acta 1993;1151:201–15.

25. Rettig WJ, Cordon-Cardo C, Koulos JP, Lewis JL, Jr., Oettgen HF,

Old LJ. Cell surface antigens of human trophoblast and choriocarcinoma defined by monoclonal antibodies. Int J Cancer 1985;35:469–75.

26. Garin-Chesa P, Campbell I, Saigo PE, Lewis JL, Jr., Old LJ, Rettig WJ. Trophoblast and ovarian cancer antigen LK26. Sensitivity and specificity in immunopathology and molecular identification as a folate-binding protein. Am J Pathol 1993;142:557–67.

27. Donaldson M, Antignani A, Milner J, et al. p47phox-deficient immune microenvironment signals dysregulate naive T-cell apoptosis. Cell Death Differ 2009;16:125–38.

28. Sonvico F, Dubernet C, Marsaud V, et al. Establishment of an *in vitro* model expressing the folate receptor for the investigation of targeted delivery systems. J Drug Deliv Sci Technol 2005;15:407–10.

29. Lu Y, Low PS. Immunotherapy of folate receptor-expressing tumors: review of recent advances and future prospects. J Control Release 2003; 91:17–29.

30. Saul JM, Annapragada A, Natarajan JV, Bellamkonda RV. Controlled targeting of liposomal doxorubicin via the folate receptor *in vitro*. J Control Release 2003;92:49–67.

31. Gerasimov OV, Boomer JA, Qualls MM, Thompson DH. Cytosolic drug delivery using pH- and light-sensitive liposomes. Adv Drug Deliv Rev 1999;38:317–38.

32. Bahlis NJ, McCafferty-Grad J, Jordan-McMurry I, et al. Feasibility and correlates of arsenic trioxide combined with ascorbic acid-mediated depletion of intracellular glutathione for the treatment of relapsed/refractory multiple myeloma. Clin Cancer Res 2002;8:3658–68.

33. Lallemand-Breitenbach V, Guillemin M-C, Janin A, et al. Retinoic acid and arsenic synergize to eradicate leukemic cells in a mouse model of acute promyelocytic leukemia. J Exp Med 1999;189:1043–52.

34. Gartenhaus RB, Prachand SN, Paniaqua M, Li Y, Gordon LI. Arsenic trioxide cytotoxicity in steroid and chemotherapy-resistant myeloma cell lines: enhancement of apoptosis by manipulation of cellular redox state. Clin Cancer Res 2002;8:566–72.

35. Baumgartner M, Sturlan S, Roth E, Wessner B, Bachleitner-Hofmann T. Enhancement of arsenic trioxide-mediated apoptosis using docosahexaenoic acid in arsenic trioxide-resistant solid tumor cells. Int J Cancer 2004;112:707–12.

36. Sturlan S, Baumgartner M, Roth E, Bachleitner-Hofmann T. Docosahexaenoic acid enhances arsenic trioxide-mediated apoptosis in arsenic trioxide-resistant HL-60 cells. Blood 2003;101:4990–7.

37. Dai J, Weinberg RS, Waxman S, Jing Y. Malignant cells can be sensitized to undergo growth inhibition and apoptosis by arsenic trioxide through modulation of the glutathione redox system. Blood 1999;93: 268–77.

38. Yang CH, Kuo ML, Chen JC, Chen YC. Arsenic trioxide sensitivity is associated with low level of glutathione in cancer cells. Br J Cancer 1999; 81:796–9.

39. Rao MV, Parekh SS, Chawla SL. Vitamin-E supplementation ameliorates chromium- and/or nickel induced oxidative stress *in vivo*. J Health Sci 2006;52:142–7.

40. Hansen JM, Zhang H, Jones DP. Differential oxidation of thioredoxin-1, thioredoxin-2, and glutathione by metal ions. Free Radic Biol Med 2006; 40:138–45.

41. Pari L, Prasath A. Efficacy of caffeic acid in preventing nickel induced oxidative damage in liver of rats. Chem Biol Interact 2008;173:77–83.

42. Sasame HA, Boyd MR. Paradoxical effects of cobaltous chloride and salts of other divalent metals on tissue levels of reduced glutathione and microsomal mixed-function oxidase components. J Pharmacol Exp Ther 1978;205:718–24.

43. Yildirim O, Buyukbingol Z. Effect of cobalt on the oxidative status in heart and aorta of streptozotocin-induced diabetic rats. Cell Biochem Funct 2003;21:27–33.

44. Dalvi RR, Robbins TJ. Comparative studies on the effect of cadmium, cobalt, lead, and selenium on hepatic microsomal monooxygenase enzymes and glutathione levels in mice. J Environ Pathol Toxicol 1978;1:601–7.

45. Shmeeda H, Mak L, Tzemach D, Astrahan P, Tarshish M, Gabizon A. Intracellular uptake and intracavitary targeting of folate-conjugated liposomes in a mouse lymphoma model with up-regulated folate receptors. Mol Cancer Ther 2006;5:818–24.